Optimal Walking of an Underactuated Planar Biped with Segmented Torso

Zhongkai Chen[1], Nafissa Lakbakbi El Yaaqoubi[2] and Gabriel Abba[2]

[1]*LCFC, Arts et Métiers ParisTech, 4 rue Augustin Fresnel, 57078 Metz Cedex 3, France*
[2]*ENIM, 1 rue Ars Laquenexy, 57078 Metz Cedex 3, France*

Keywords: Biped Robot, Optimal Walk, Segmented Torso, Zero Dynamics, Energy Efficiency.

Abstract: Recently, underactuated bipeds with pointed feet have been studied to achieve dynamic and energy efficient robot walking patterns. However, these studies usually simplify a robot torso as one link, which is different from a human torsos containing 33 vertebrae. In this paper, therefore, we study the optimal walking of a 6-link planar biped with a segmented torso derived from its 5-link counterpart while ensuring that two models are equivalent when the additional torso joint is locked. For the walking, we suppose that each step is composed of a single support phase and an instantaneous double support phase, and two phases are connected by a plastic impact mapping. In addition, the controlled outputs named symmetry outputs capable of generating exponentially stable orbits using hybrid zero dynamics, are adopted to improve physical interpretation. The desired outputs are parameterized by Bézier functions, with 5-link robot having 16 parameters to optimize and 6-link robot having 19 parameters. According to our energy criterion, the segmented torso structure may reduce energy consumption up to 8% in bipedal walking, and the maximum energy saving is achieved at high walking speeds, while leaving the criteria at low walking speeds remain similar for both robots.

1 INTRODUCTION

One of the fundamental tasks in designing biped robots is to find robot structures and control strategies capable of providing energy-efficient and stable walking motions. As indicated in Figure 1, many researchers have tried to study the energy saving benefits of bionic robot designs by adopting certain human resembling parts such as curved feet (Martin and Schmiedeler, 2012), rolling knees (Hobon et al., 2013), locked knees (Sinnet et al., 2011), swinging arms (Kaddar et al., 2012) or springs (Bauer et al., 2014). Nevertheless, the theoretical advantages of a human-like robot torso are still rarely studied among the vast literature on humanoid robots, despite the studies on realizing human-like biped torsos from a practical point of view (Mizuuchi et al., 2006).

Unveiling the theoretical advantages of humanlike robot structures requires numerical optimization. By far, the most common method is through designing reference trajectories with a limited number of parameters, whether the trajectories are functions of time or functions of robot state, and then optimizing these parameters using a certain cost function. Many researchers have used optimization in the analysis
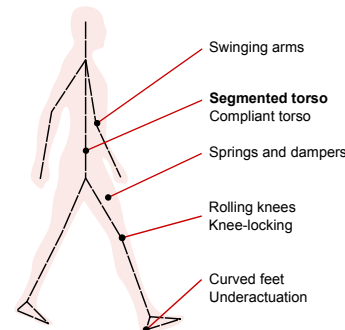

Figure 1:   Possible methods for reducing energy consumption.

and design of biped walking motions with trajectories defined as functions of time (Cabodevila and Abba, 1997; Chevallereau and Aoustin, 2001; Beletskii et al., 1982), and these early studies usually adopted the zero moment point (ZMP) principle to ensure the feasibility of various walking motions. However, a periodic and feasible walking motion might not be stable because biped robots are hybrid systems with impacts during each step, which might serve as a discrete positive feedback of error. Some researchers also attempted to eliminate the impact completely and thus creating walking motions that consume no

mechanical energy, but these studies are only valid for passive biped robots walking in a highly controlled environment (Rouhollah et al., 2013). For activated robots with motors, it's practically impossible to eliminate the energy consumption caused by Joule heating.

Recently, with more and more researchers striving to achieve more dynamic biped walking patterns, a planar biped robot with pointed feet and the name "RABBIT" was created, which witnessed the birth of the concept called "virtual constraints" (Chevallereau et al., 2003). By using a monotonic scalar quantity representing the progression of a step, Westervelt and Grizzle (2002) proposed a method to define trajectory functions with a closed-form stability indicator. Armed with this method, Ames (2012) proposed human outputs to relate the walking motions of biped robots to the human walking data collected in a laboratory.

The work presented here is inspired by both the previously studied human-like parts and the optimization methods with provable stability. Our intention is to analyze the energy-saving potentials of the segmented torso. The optimal walking of a 5-link robot and a 6-link robot with underactuated pointed feet is studied to quantify the difference between these two robot configurations. The segmented torso of the 6-link robot is assumed to be straight at the beginning and the end of each step. Based on the stability analysis proposed by Westervelt and Grizzle (2002), we define symmetry outputs to observe the mirror-like behavior of a virtual stance leg and a virtual swing leg. This interpretation of bipedal walking motions is related to a previous research on asymptotic stable walking with simplified posture control and swing leg advancement strategies (Grizzle et al., 2001). By running optimization with symmetry outputs at different walking speeds, we have found obvious energy efficiency improvement of the 6-link robot compared with its 5-link rival, especially at high walking speeds.

The paper is structured as follows. Section 2 delineates the biped models of both 5-link and 6-link robots. Section 3 introduces the symmetry outputs together with the feedback design using optimized HZD. Section 4 deals with the optimization problem using Bézier trajectories with provable stability. Section 5 presents the optimized walking motions of the two biped robots at different speeds. Finally, Section 6 concludes this paper by discussing the advantage of the additional torso joints and possible subsequent studies.

2 ROBOT MODELS

2.1 Robot Parameters

Both 5-link robot and 6-link robot have pointed feet which are not actuated during each step, and the rotor inertias are the same for all the actuators. As shown in Figure 2, the 5-link robot analyzed here comprises one torso, two femurs and two tibiae. We assume that all links are considered rigid and the motion is constrained to the sagittal plane.
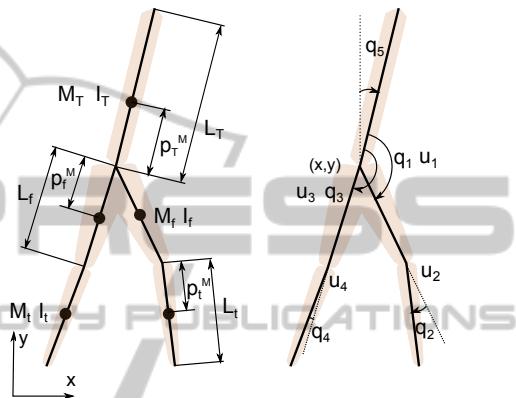

Figure 2: 5-link planar biped robot.

The 6-link robot, depicted in in Figure 3, is derived from the 5-link robot, and the only difference is that the additional torso joint divides the torso into an upper torso and a lower torso. In order to compare the performance of both robots, the 6-link robot should be equivalent to its 5-link counterpart once the additional joint is locked. This is realized by the following equations

$$M_T = M_{T1} + M_{T2} \tag{1}$$

$$M_T p_T^M = M_{T1} p_{T1}^M + M_{T2}(L_{T1} + p_{T2}^M) \tag{2}$$

$$
\begin{aligned}
I_T = & I_{T1} + M_{T1}(p_T^M - p_{T1}^M)^2 \\
& + I_{T2} + M_{T2}(p_T^M - p_{T2}^M)^2
\end{aligned} \tag{3}
$$

where the notations used above is explained in Table 1. For the actuators of the femurs and tibiae, the rotor inertias equal $0.83\ kgm^2$, and the motor rotor inertia of the additional torso joint is $0.2\ kgm^2$.

2.2 Dynamic Models

The generalized coordinate vector describing both biped robots in the sagittal plane is defined as $q_e = [x, y, q_1, q_2, ..., q_n]'$ where $n = 5$ or 6 equaling the number of links. It contains two coordinates (x and y) describing the position of pelvis and n angles $q = [q_1, q_2, ..., q_n]'$ for the orientation of legs and torsos. We assume that the positive angles are anticlockwise.

Table 1: Model Parameters for 5-link Robot and 6-link Robot.

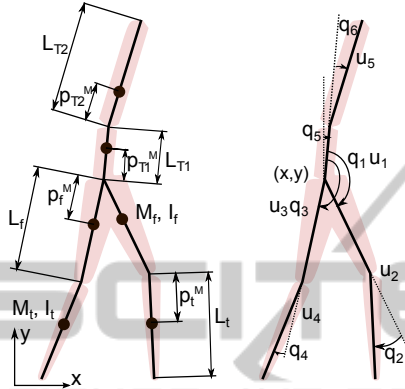| Model Parameters	Common		5-link	6-link	
	Femurs(f)	Tibia(t)	Torso(T)	Lower Torso($T1$)	Upper Torso($T2$)
Mass,$M_*(kg)$	6.8	3.2	17.1	10	7.1
Length,$L_*(m)$	0.4	0.4	0.625	0.3	0.325
Inertia,$I_*(m^2kg)$	0.0693	0.0484	0.562	0.115	0.075
Mass Center,$p_*^M(m)$	0.163	0.127	0.224	0.1	0.1

Figure 3: 6-link planar biped robot.

The dynamic model of the biped robot is divided into two models: the swing phase model and the impact model. Using the Euler-Lagrange equations, one obtains the swing phase models of the form

$$D(q)\ddot{q} + C(q,\dot{q}) + G(q) = Bu \qquad (4)$$

where the matrix D is the inertia matrix, C is the $(n \times 1)$ vector of Coriolis terms, G is the $(n \times 1)$ vector of gravity terms, and B maps the joint torques to generalized forces.

An impact occurs when the swing leg end hits the ground. We assume that the impact is plastic, and the relabeling of robot's coordinates after each impact is also included in the impact model. Let $x = [q,\dot{q}]'$ be the state variables of the robot. The impact model can be formulated as

$$x^+ = \Delta(x^-) = \begin{bmatrix} \Delta_q q^- \\ \Delta_{\dot{q}}(q^-)\dot{q}^- \end{bmatrix} \qquad (5)$$

where Δ_q is a relabeling function, $\Delta_{\dot{q}}(q^-)$ is a $n \times n$ matrix, $x^+ = [q^+,\dot{q}^+]'$ and $x^- = [q^-,\dot{q}^-]'$ (Westervelt and Grizzle, 2002).

The overall model of walking is obtained by combining the swing phase model and the impact model to form a hybrid model. Assuming that the evolution of the swing phase model possesses finite left and right limits, one can denote them by $x^-(t) = lim_{\tau \to t^-} x(\tau)$ and $x^+(t) = lim_{\tau \to t^+} x(\tau)$, respectively. The hybrid model can then be formulated as

$$\Sigma : \begin{cases} \dot{x} = f(x) + g(x)u & x \notin S \\ x^+ = \Delta(x^-) & x^- \in S \end{cases} \qquad (6)$$

where $S = \{(q,\dot{q})|h_{sw}(q) = 0, dh_{sw}(q)\dot{q} < 0\}$ is the switching surface.

Converting the dynamic equation (4) to a first order ODE, $f(x)$ and $g(x)$ can be calculated as

$$f(x) = \begin{bmatrix} \dot{q} \\ -D^{-1}(q)(C(q,\dot{q}) + G(q)) \end{bmatrix} \qquad (7)$$

$$g(x) = \begin{bmatrix} 0_{5\times4} \\ D^{-1}B \end{bmatrix} \qquad (8)$$

3 OUTPUTS AND FEEDBACK

3.1 Symmetry Outputs

Depending on the robot model one chooses, the dimension of the output equals to $(n-1)$, and an almost linear output function can be defined as

$$y = h(q) = h_0(q) - h_d \circ \theta(q) \qquad (9)$$

where $h_0(q)$ represents independent controlled quantities and $h_d \circ \theta(q)$ represents the ideal evolution of these quantities as a function of the scalar quantity $\theta(q)$ (Westervelt et al., 2007). $\theta(q)$ is a strictly monotonic function of the robot's state, and it is used to replace time in parameterizing periodic biped motion. If the virtual stance leg is defined as the line connecting both the stance hip and the stance foot, then its opposite angle in the sagittal plane will be monotonically increasing. Since the lengths of the femurs and the tibiae are equal, θ can be formulated for both robots as

$$\theta(q) = cq = -q_1 - q_2/2 - q_5 \qquad (10)$$

where the minus signs are adopted to make θ strictly increasing.

Intuitively, there are two tasks to achieve in bipedal walking: posture control and swing leg advancement. Posture control is to maintain the torso in an almost upright position, while swing leg advancement deals with commanding the swing leg to pass beyond the stance leg and ensuring a desired step length. For a compass gait robot with no ankles and no knees, the simplest version of posture control is to maintain torso at some constant value, and

the simplest version of swing leg advancement is to command the swing leg to behave as the mirror image of the stance leg (Grizzle et al., 2001). Inspired by the physical interpretation of these methods, we define h_0 of the 5-link robot as follows

$$h_0(q) = H_0 q = [\theta_{symm}, q_2, q_4, q_5]' \qquad (11)$$

$$\theta_{symm} = q_1/2 + q_2/4 + q_3/2 \\ + q_4/4 + q_5 + \pi \qquad (12)$$

where θ_{symm} describes the mirror-like behavior of the virtual swing leg with regard to the virtual stance leg. As shown in Fig.4, it can be interpreted physically as the angle between the bisector of virtual swing leg and virtual stance leg and the gravity direction. q_5 is the absolute angle of the torso, which is responsible for posture control. q_2 and q_4 are the angles of the stance knee and the swing knees. Since the outputs have the same proportion of quantities from the stance leg (q_1, q_2) and the swing leg (q_3, q_4), it is named as "Symmetry Ouputs". As for h_d, its definition is related to specific feedback designs, which will be discussed in the next section. For 6-link robot, the definition of θ_{symm} is the same, but $h_0(q)$ need to be replaced by $[\theta_{symm}, q_2, q_4, q_5, q_6]'$.
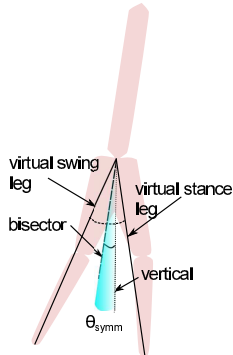

Figure 4: Geometric interpretation of symmetry outputs.

3.2 Feedback Design using HZD

Assuming that h_d is defined by trajectory functions of $\theta(q)$ and the invariance of the impact map is satisfied, the goal of the feedback design with optimized HZD is to keep the robot evolution on the zero dynamic surface. The method of explicitly constructing the zero dynamics already exists, and we briefly list all the equations with the same labeling system in the context of our robot configuration so as to achieve logical completion (Westervelt et al., 2003). The following equations can be used in calculating zero dynamics for both the 5-link robot and the 6-link robot.

Because of the specific choice of $h_0(q)$, one can express the zero dynamics as

$$\begin{aligned} \xi_1 &= \theta(q) \\ \xi_2 &= \gamma(q, \dot{q}) \end{aligned} \qquad (13)$$

where $\theta(q)$ is defined by (10) and $\gamma(q, \dot{q})$ can be explicitly computed to be the fifth entry of $D(q)\dot{q}$. The hybrid zero dynamics is originally 2-dimensional, and it can be equivalent to a 1-dimensional discrete time dynamical system when the hyperplane $\xi_1 = \theta_1^-$ is chosen as the Poincaré section and the coordinate transformation $\zeta_2 = \frac{1}{2}(\xi_2)^2$ is adopted, yielding

$$\frac{d\zeta_2}{d\xi_1} = \frac{\kappa_2(\xi_1)}{\kappa_1(\xi_1)} \qquad (14)$$

where $\kappa_1(\xi_1)$ and $\kappa_2(\xi_1)$ are given by

$$\kappa_1(\xi_1) = \frac{\partial \theta}{\partial q} \begin{bmatrix} \frac{\partial h}{\partial q} \\ \gamma_0 \end{bmatrix}^{-1} \begin{bmatrix} 0 \\ 1 \end{bmatrix} \Bigg|_Z \qquad (15)$$

$$\kappa_2(\xi_1) = -\frac{\partial V}{\partial q_5} \Bigg|_Z \qquad (16)$$

with $V(q)$ the potential energy of the biped, $\gamma_0 = D_5$ (the fifth row of D) and $\partial V/\partial q_5 = G_5$ (the fifth row of $G(q)$).

The zero dynamic representation enables us to determine the existence and stability of a fixed point of the zero dynamics without integrating the ODE (Westervelt et al., 2007). To begin with, the relation between ξ_2^- and ξ_2^+ can be calculated by

$$\xi_2^+ = \delta_{zero} \xi_2^- \qquad (17)$$

where δ_{zero} intricately determines the stability of a limit cycle in the zero dynamics surface and can be computed in advance as

$$\delta_{zero} = \gamma_0(q^+) \Delta_{\dot{q}}(q_0^-) \sigma_{\dot{q}}(q_0^-) \qquad (18)$$

$$\sigma_{\dot{q}}(q_0^-) = \begin{bmatrix} \frac{\partial h}{\partial q}(q_0^-) \\ \gamma_0(q_0^-) \end{bmatrix}^{-1} \begin{bmatrix} 0 \\ 1 \end{bmatrix} \qquad (19)$$

Thus the potential energy of the zero dynamics (13) becomes

$$V_{zero}(\xi_1) = -\int_{\theta^+}^{\xi_1} \frac{\kappa_2(\xi)}{\kappa_1(\xi)} d\xi \qquad (20)$$

which can determine whether the biped will take a full step by judging if

$$\frac{\delta_{zero}^2}{1 - \delta_{zero}^2} V_{zero}(\theta^-) + K < 0, (\delta_{zero}^2 \neq 0) \qquad (21)$$

where $K = \max V_{zero}(\xi_1)$ with $\theta^+ \leq \xi_1 \leq \theta^-$.

Furthermore, if $0 < \delta_{zero} < 1$ also holds, there exists an exponentially stable periodic orbit with the fixed point being

$$\xi_1^* = cq_0^-|_{\Psi_p^-}, \zeta_2^* = \frac{-V_{zero}(\theta^-)}{1 - \delta_{zero}^2} \qquad (22)$$

Given ξ_1^* and ζ_2^*, $\xi_2(\xi_1, \zeta_2^*)$ can be further calculated by

$$\xi_2(\xi_1, \zeta_2^*) = -\sqrt{2(\delta_{zero}^2 \zeta_2^* - V_{zero}(\xi_1))} \qquad (23)$$

Then $q(t)$ and $\dot{q}(t)$ are given by

$$q = \begin{bmatrix} H_0 \\ c \end{bmatrix}^{-1} \begin{bmatrix} h_d(\xi_1) \\ \xi_1 \end{bmatrix} \qquad (24)$$

$$\dot{q} = \begin{bmatrix} \frac{\partial h}{\partial q} \\ \gamma_0 \end{bmatrix}^{-1} \begin{bmatrix} 0 \\ \xi_2 \end{bmatrix} \qquad (25)$$

and the torque $u(x)$ is attained through

$$u(x) = -(L_g L_f h(q, \dot{q}))^{-1} L_f^2 h(q, \dot{q}) \qquad (26)$$

In addition, $t(\xi_2)$ can be calculated as

$$t(\xi_2) = \int_{\theta^+}^{\theta^-} \frac{1}{\kappa_1(\xi_1)\xi_2(\xi_1, \xi_2^-)} d\xi_1 \qquad (27)$$

4 OPTIMAL WALKING MOTION

4.1 Parameterization of h_d

Bézier polynomials are widely adopted in parameterizing underactuated biped robots because they do not display large oscillations with small parameter variations and they can easily achieve impact invariance (Westervelt et al., 2007).

To facilitate calculation, we start by normalizing the previously defined $\theta(q)$ as

$$s(q) = \frac{\theta(q) - \theta^+}{\theta^- - \theta^+} \qquad (28)$$

with θ^+ the minimum value of $\theta(q)$ and θ^- the maximum value of $\theta(q)$. Then $h_d \circ \theta(q)$ can be defined as

$$h_d \circ \theta(q) = B_Z \circ s(q) \qquad (29)$$

where $B_Z = [b_1, ... b_{n-1}]'$ with n being the number of links as before. Each b_i is further defined by

$$b_i(s) = \sum_{k=0}^{5} a_k^i \frac{5!}{k!(5-k)!} s^k (1-s)^{5-k} \qquad (30)$$

which is a Bézier polynomial of degree 5. Group the parameters a_k^i into vectors as $a_k = (a_k^1, a_k^1, ..., a_k^{n-1})$, and we can calculate a_0 directly from a_5 using

$$\begin{bmatrix} a_0 \\ \theta^+ \end{bmatrix} = H \Delta_q H^{-1} \begin{bmatrix} a_5 \\ \theta^- \end{bmatrix} \qquad (31)$$

where $H = [H_0', c']'$. Moreover a_1 can also be calculated once a_5 and a_4 are available simply by using

$$a_1 = \frac{\theta^- - \theta^+}{5c\dot{q}^+} H_0 \dot{q}^+ + a_0 \qquad (32)$$

where $\dot{q}^- = \sigma_{\dot{q}}(q_0^-)$ and $\dot{q}^+ = \Delta_{\dot{q}}(q_0^-)\dot{q}^-$.

Thus the parameter set $\{a_2, a_3, a_4, a_5\}$ is able to determine h_d for both the 5-link and 6-link robot. For the 5-link robot, the parameter set contains 16 parameters. As for the 6-link robot, the torso has the tendency to bend down significantly at high walking speeds, which impairs its resemblance to real human torsos. In order to avoid excessive curvy torsos, we assume that the initial shape of the segmented torso is straight ($q_6^- = 0$), meaning that there will be one less parameter to optimize. Therefore, the parameter set of the 6-link robot is composed of 19 parameters.

4.2 Cost Function

For the system (6), the output (9) is defined by h_0, h_d and θ as in (10), (11) and (29). The optimization requires one to find an appropriate cost function. For biped robots with electrical motors, the major energy consumption is caused by Joule effect, and thus the cost function should be proportional to this loss of energy. It is defined as the integral of the norm of the torque for a displacement of one meter

$$C = \frac{1}{d_s} \int_0^T \sum_{i=1}^{N-1} (u_i^*(t))^2 dt \qquad (33)$$

where T is the step duration, and d_s corresponds to step length. The cost function can also be written as (Westervelt and Grizzle, 2002)

$$C = \frac{1}{d_s} \int_{\theta^+}^{\theta^-} \frac{\sum_{i=1}^{N-1} (u_i^*(\xi_1, \xi_2))^2}{\kappa_1(\xi_1)\xi_2(\xi_1, \xi_2^-)} d\xi_1 \qquad (34)$$

4.3 Constraints

The constraints in the optimization problem is adopted to ensure the validity of the optimal trajectory. For both robot configurations, the constraints include:

- The ground reaction acting on the stance leg end should always be larger than $50N$, and the maximum ratio of tangential to normal ground reaction forces should be less than the friction coefficient, which is 0.6 in our case.

- The impulsive impact force must be upward and conform to the friction coefficient. The post-impact velocity of the swing leg tip is upward.

- The swing leg end must not touch the ground before the end of one periodic step.

- The existence of a fixed point needs $\xi_2^* > K/\delta_{zero}^2$ and the stability of the fixed point, $0 < \delta_{zero}^2 < 1$.

- The average walking speed, $v = d/T$.

4.4 Optimization Method

The above procedure can be performed using MATLAB Optimization toolbox, which provides different optimization methods such as Nelder-Mead, sequential quadratic programming (SQP), and active set. Among them, we have chosen SQP as our optimization method for its superior capability in handling the situation where the cost function cannot provide the criterion due to the violation of certain constraints such as the constraint ensuring the existence of a fixed point.

5 RESULT ANALYSIS

As the stability of the hybrid zero dynamics is well defined, we no longer need to use simulation to prove the stability of the walking. In order to compare the energy efficiency between the 5-link robot and 6-link robot, we have run optimization at various speeds ranging from 0.25m/s to 1.5m/s. As depicted in Figure 5, the torque costs of the two biped robots are almost the same at the walking speed from 0.25m/s to 1.2m/s. As the walking speed continues to increase, the advantage of the 6-link robot in energy efficiency becomes more and more obvious. The similar results were also obtained in biped robots with modest swinging arms, but their method is based on ZMP theories and thus do not provide solid proof of stability (Kaddar et al., 2012).

At 1.5m/s, the torque cost of the 6-link robot is almost 8% less than that of its counterpart. The stick diagrams of the both robots walking at this speed are illustrated in Figure 6 and Figure 7 respectively, and the friction requirements for both walking motions are satisfied according to Figure 8. The torque charts for
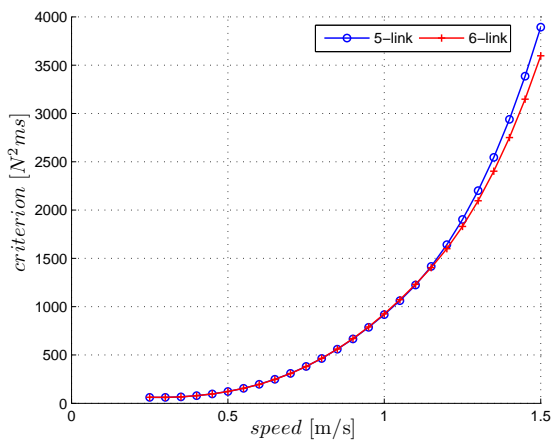

Figure 5: The torque cost versus walking speed for both biped robots.
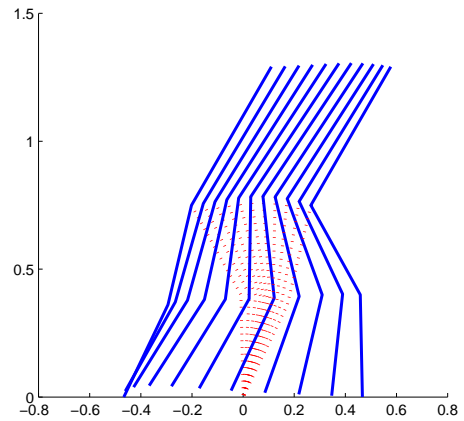

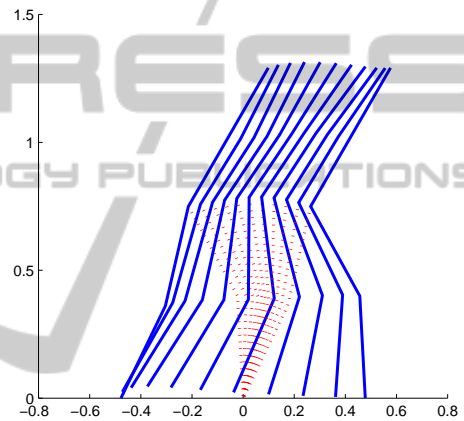Figure 6: The optimal walking motion of the 5-link robot at 1.5m/s.

Figure 7: The optimal walking motion of the 6-link robot at 1.5m/s.

all the actuators are shown in Figure 9. We can see that the gaits of these two robots are quite similar. As shown in Table 2, the additional torso joint do consume energy, but on the whole the 6-link robot is still more energy efficient because of the reduced torque costs at the other joints, especially at the swing hip. The angle charts describing the movement of both robots are shown in Figure 10. We can find that the fluctuation of q_5 and θ_{symm}, for both robots, is comparatively mild compared with all the other angles. The intuitive justification for it would be that the torso rotation is limited during one step and the virtual swing leg behave approximately as the mirror image of the virtual stance leg.

6 CONCLUSIONS

The advantage of using a segmented torso instead of a one-piece torso is studied in this paper. According to the current optimization results, the 6-link biped robot

Table 2: Energy Costs at 1.5m/s.

Robot Type	Energy Costs (N^2ms)					
	Stance Hip	Stance Knee	Swing Hip	Swing Knee	Torso Joint	Total
5-link	1634	364.7	1579	314.5	-	3893
6-link	1689	266.0	1301	269.2	64.8	3590
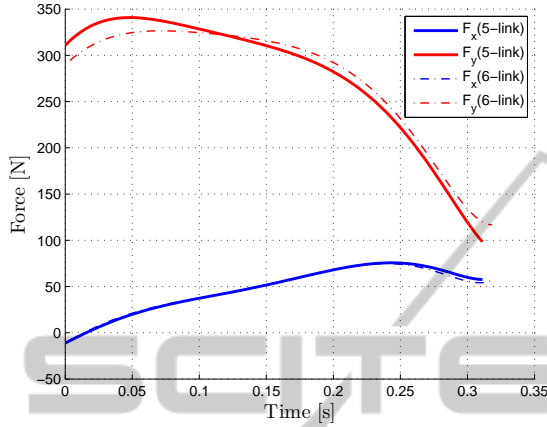
Figure 8: The ground reaction forces versus time.

Figure 10: The angles versus time.

Figure 9: The applied torques versus time.

on exploring the effect of a passive segmented torso on the energy efficiency of walking motion.

ACKNOWLEDGEMENTS
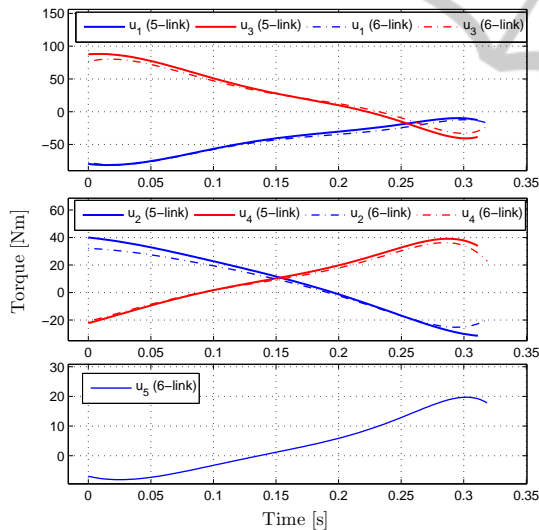
with segmented torso consumes less energy than its 5-link counterpart at high walking speeds, and the improvement is mainly due to the reduced torque cost at the swing hip. The results are purely theoretical since there is no platform capable of testing 6-link biped with the additional torso joint at present, but we will try to attain related experimental data in the future. In addition, there may still be room for further reducing the energy criterion because the current hypotheses of the additional torso joint is still different from the semi passive nature of a real human torso. Therefore, our future study will focus
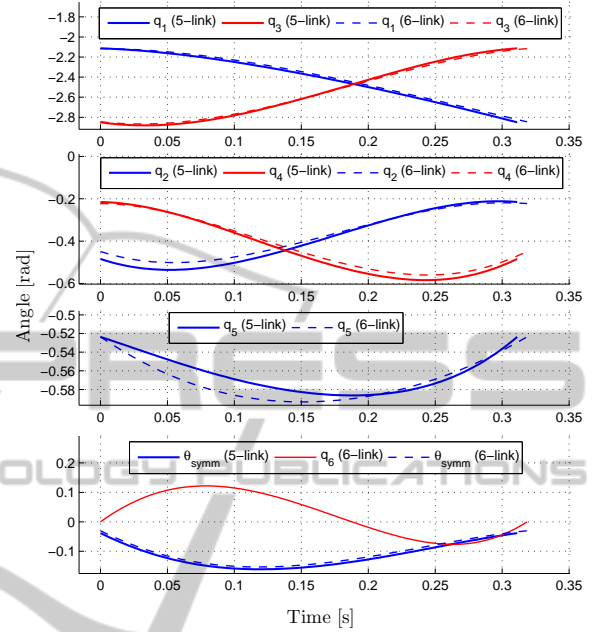
REFERENCES

Ames, A. (2012). First steps toward underactuated human-inspired bipedal robotic walking. In *Proceedings - IEEE International Conference on Robotics and Automation*, pages 1011–1017.

Bauer, F., Fidlin, A., and Seemann, W. (2014). Energy efficient bipedal robots walking in resonance. *ZAMM - Journal of Applied Mathematics and Mechanics / Zeitschrift für Angewandte Mathematik und Mechanik*.

Beletskii, V., Berbyuk, V., and Samsonov, V. (1982). Parametric optimization of motions of a bipedal walking robot. *Mechanics of solids*, 17(1):24–35.

Cabodevila, G. and Abba, G. (1997). Quasi optimal gait for a biped robot using genetic algorithm. In *Proceedings of the IEEE International Conference on Systems, Man and Cybernetics*, volume 4, pages 3960–3965.

Chevallereau, C., Abba, G., Aoustin, Y., Plestan, F., Westervelt, E., Canudas-de Wit, C., and Grizzle, J. (2003). Rabit: A testbed for advanced control theory. *IEEE Control Systems Magazine*, 23(5):57–79.

Chevallereau, C. and Aoustin, Y. (2001). Optimal reference trajectories for walking and running of a biped robot. *Robotica*, 19(5):557–569.

Grizzle, J., Abba, G., and Plestan, F. (2001). Asymptotically stable walking for biped robots: Analysis via systems with impulse effects. *IEEE Transactions on Automatic Control*, 46(1):51–64.

Hobon, M., Elyaaqoubi, N., and Abba, G. (2013). Gait optimization of a rolling knee biped at low walking speeds. In *ICINCO 2013 - Proceedings of the 10th International Conference on Informatics in Control, Automation and Robotics*, volume 2, pages 207–214.

Kaddar, B., Aoustin, Y., and Chevallereau, C. (2012). Arms swing effects on a walking planar biped. In *ASME 2012 11th Biennial Conference on Engineering Systems Design and Analysis, ESDA 2012*, volume 3, pages 293–301.

Martin, A. and Schmiedeler, J. (2012). The effects of curved foot design parameters on planar biped walking. In *Proceedings of the ASME Design Engineering Technical Conference*, volume 4, pages 815–824.

Mizuuchi, I., Yoshikai, T., Sodeyama, Y., Nakanishi, Y., Miyadera, A., Yamamoto, T., Niemelä, T., Hayashi, M., Urata, J., Namiki, Y., Nishino, T., and Inaba, M. (2006). Development of musculoskeletal humanoid kotaro. In *Proceedings - IEEE International Conference on Robotics and Automation*, volume 2006, pages 82–87.

Rouhollah, J., Louis, L., Aren, H., and Ranjan, M. (2013). Energy-conserving gaits for point-foot planar bipeds: A five-dof case study. In *ASME 2013 Dynamic Systems and Control Conference*.

Sinnet, R., Powell, M., Shah, R., and Ames, A. (2011). A human-inspired hybrid control approach to bipedal robotic walking. In *IFAC Proceedings Volumes (IFAC-PapersOnline)*, volume 18, pages 6904–6911.

Westervelt, E. and Grizzle, J. (2002). Design of asymptotically stable walking for a 5-link planar biped walker via optimization. In *Proceedings - IEEE International Conference on Robotics and Automation*, volume 3, pages 3117–3122.

Westervelt, E., Grizzle, J., and Koditschek, D. (2003). Hybrid zero dynamics of planar biped walkers. *IEEE Transactions on Automatic Control*, 48(1):42–56.

Westervelt, E. R., Grizzle, J. W., Chevallereau, C., Choi, J. H., and Morris, B. (2007). *Feedback Control of Dynamic Bipedal Robot Locomotion*. Taylor & Francis LLC, first edition.